Synthesis of pyridine and picolines over Co-modified HZSM-5 catalyst

Yumin Liu [a,b], Heqin Yang [a], Fang Jin [a], Yue Zhang [a], Yongdan Li [a,*]

[a] *Tianjin Key Laboratory of Applied Catalysis Science and Technology, School of Chemical Engineering and Technology,
Tianjin University, Tianjin 300072, China*
[b] *College of Chemical and Pharmaceutical Engineering, Hebei University of Science and Technology, Shijiazhuang 050018, China*

Abstract

Co-modified HZSM-5 zeolite catalysts were prepared by ion exchange with $Co(CH_3COO)_2$ solution, and incipient wetness impregnation with aqueous solutions of $Co(NO_3)_2$ and $Co(CH_3COO)_2$, respectively. The catalysts were characterized by N_2-adsorption, NH_3–TPD, FTIR and adsorption of *m*- and *p*-cresol. The catalytic performance for the synthesis of pyridine and picolines from aldehyde-ammonia condensation was tested. It shows that Co disperses in the zeolite pores for the ion exchanged samples, while Co deposits mainly on the external surface for the samples prepared by impregnation of $Co(CH_3COO)_2$, which results in a narrowing of the pore mouth. NH_3–TPD and pyridine-FTIR measurements indicate that the total acidity and the Lewis acidity of the catalysts increased with the decrease of Brönsted acidity among the samples. The samples prepared by impregnation with $Co(CH_3COO)_2$ have the highest yield of the desired products among all the samples tested. This is attributed to the change of surface acidity and the reduction of the pore-mouth of the zeolite.
© 2007 Elsevier B.V. All rights reserved.

Keywords: Pyridine; Picolines; Zeolite; HZSM-5; Surface acid sites

1. Introduction

Pyridine and picolines are useful intermediates in the synthesis of herbicides, pharmaceuticals and surfactants [1]. On commercial scale, pyridine and picolines are synthesized from aldehydes-ammonia condensation over an amorphous aluminosilicate catalyst promoted by ThO_2, ZnO or CdO with 40–60% yield [1]. These catalysts have common drawbacks such as poor catalytic activity, selectivity, thermal stability and regeneration capacity. Recently, crystalline aluminosilicate catalysts began to replace the amorphous ones, because of their better thermal stability, special surface acidity and regular pore structure.

The strong acidity and profound shape selectivity make ZSM-5 a promising catalyst for the reaction [2–4]. Previous work proved that a suitable acidity is required for the reaction [1]. The compensating cations in the zeolite are found to have influence on the catalytic behavior and extensive works have been done on their modification effect [2,3,5–7]. However, a good catalyst and a deep fundamental understanding on the reaction are still needed.

In this work, the effect of the techniques for Co incorporation into HZSM-5 is investigated. The effect of the preparation parameters on the acidity, pore-mouth opening and catalytic performance are discussed.

2. Experimental

2.1. Catalyst preparation

Three series of catalysts containing Co were prepared using HZSM-5 zeolite, with Si/Al = 70 atom/atom and calcined at 873 K for 5 h, as a starting material. The further preparation procedures were as follows:

The As samples: Co was incorporated by an ion-exchange technique, in which 15 g HZSM-5 was added into 300 ml solution with $Co(CH_3COO)_2$ at different concentration. After 10 h stirring at 363 K, the slurry was filtrated and washed with distilled water. The Bs samples: Co was incorporated by incipient wetness impregnation with a $Co(NO_3)_2$ aqueous solution. The Cs samples were prepared by using $Co(CH_3COO)_2$ solution under the same conditions.

After drying at 393 K for 16 h, all the samples were calcined under O_2 flow at 773 K. The chemical compositions of the As samples determined by ICP(ICP-9000(N + M)) analysis

* Corresponding author. Tel.: +86 2227405613; fax: +86 2227405243.
E-mail address: ydli@tju.edu.cn (Y. Li).

Table 1
The Co content of samples As

Samples, As	Co content %
A1	0.091
A2	0.51
A3	1.04
A4	1.78

are listed in Table 1. For the Bs and Cs samples, a same Co content with As for the samples with a same subscription number was assumed, because of the stoichiometric addition of the element in the incipient wetness method.

2.2. Catalyst characterization

X-ray diffraction (XRD) patterns were recorded on a Panalystical X'Pert Pro diffractometer with Co Kα radiation. NH$_3$–temperature programmed desorption (NH$_3$–TPD) was performed in a quartz micro-reactor. A 0.12 g of catalyst was heated in argon flow at 823 K for 0.5 h. Afterwards it was cooled down to 393 K, NH$_3$ was then introduced. The sample was swept with argon at 393 K for 2 h. TPD was then carried out with an argon flow at a rate of 40 ml/min (STP) from 393 to 923 K with a heating rate of 10 K/min. The thermal conductivity signal was recorded. The pyridine adsorption Fourier transform-infrared (FTIR) spectroscopy was carried out with a Vector 22 spectrometer using self-supporting wafers, ≈10 mg cm^{-2}, which were activated in vacuum at 473 K. Before recording the spectra, pyridine was adsorbed at 473 K and the apparatus was evacuated for 1 h. A PHILIPS XL 30 ESEM scanning electron microscope (SEM) equipped with an energy dispersive X-ray spectrometer (EDX) was used. The selective adsorption experiments of *p*-cresol and *m*-cresol were carried out using 1,3,5-trimethylbenzene as solvent under static conditions. The catalyst used was pretreated at 773 K for 5 h and was then immersed in a solution of *p*-cresol s and *m*-cresol (1:1) at 303 K for 48 h, respectively.

2.3. Activity measurements

The reactions were done in a fixed bed tubular reactor with 10 mm diameter in the conditions of 723 K, time on stream 2 h and atmospheric pressure, 1.25 g of catalyst with 0.18–0.25 mm diameter was used. In a typical exper-

iment, the catalyst was heated up to 723 K under nitrogen flow for 1 h and then the system was stabilized at 723 K for 0.5 h. Formaldehyde/acetaldehyde 2:3 mol mol^{-1}, ammonia/aldehydes 2:1 mol mol^{-1} were introduced into the reactor at liquid WHSV 2.86 h^{-1}. The product was collected 5 min later with a condenser and was analyzed by a GC equipped with a FID using a HP-5 column. The product was confirmed by GC–MS.

3. Results and discussion

3.1. The structure of catalyst

The XRD patterns of samples A3, B3 and C3 show no remarkable differences, indicating no destruction of the zeolite structure during the three different preparation procedures. No Co containing phases were detected, which means that Co is highly dispersed.

The pore structure of the prepared samples was characterized by the selective adsorption experiments. Probe molecules *p*-cresol and *m*-cresol, with kinetic diameters 0.58 nm and 0.63 nm, were employed, respectively. It was reported that the pore mouth dimensions of the two kinds of channels in HZSM-5 are 0.56 nm × 0.54 nm and 0.57 nm × 0.51 nm, respectively. Table 2 summarizes the adsorption capacity data of all the samples. It shows that the parent HZSM-5 adsorption ability to *p*-cresol is similar to that of the *m*-cresol. A reduction of the total adsorption capacity both for *p*- and *m*-cresol along with the increase of Co content is observed for all the three series of samples. The adsorption capacity of *p*-cresol shows an order as HZSM-5 > As > Cs > Bs, which indicates that Co introduced by ion exchange (As) have the smallest effect on the pore channels of the zeolite. On the contrary, the impregnation method with Co(NO$_3$)$_2$ have obvious influence on their pore structure. For the As samples, a slight increase of *p-/m*-cresol with the increase of Co content is noticed. This demonstrates that the pore structure of As have no obvious change. In the case of the Bs samples, the adsorption capacity of *p*- and *m*-cresol both shows a significant loss along with the increase of the Co content, while the *p-/m*-cresol ratio shows rather constant. This indicates that there might be a narrowing of pore channel and a decrease of the pore volume. For the Cs samples, the adsorption of *m*-cresol is significantly inhibited, however, the adsorption amount of *p*-cresol has a little loss. The ratio of the *p-/m*-cresol adsorption increased, which shows that there is an irregular dis-

Table 2
Adsorption properties of different modified HZSM-5 catalysts

Sample no.	Adsorption capacity (%)								
	p-cresol			*m*-cresol			*p*-cresol/*m*-cresol		
	Series As	Series Bs	Series Cs	Series As	Series Bs	Series Cs	Series As	Series Bs	Series Cs
HZSM-5	6.39			6.31			1.00		
2	6.30	5.71	6.28	6.15	5.36	5.15	1.02	1.07	1.22
3	6.23	5.37	6.20	5.94	5.07	4.90	1.05	1.06	1.27
4	6.15	5.00	6.13	5.84	4.71	4.74	1.05	1.05	1.29

Table 3
The Co content on the surface of catalysts determined by EDX

Co content (wt%)	Co on the surface (wt%)		
	Series As	Series Bs	Series Cs
0.51	0.32	0.33	0.38
1.78	1.50	1.32	1.83

tribution of Co compound on the surface of ZSM-5. It is likely that the Co incorporated by impregnation of $Co(CH_3COO)_2$ has a preference of pore mouth deposition, which narrows the mouth, but may not change the intracrystalline pore space.

The Co distribution on the external surface of six samples measured by EDX is given in Table 3. It shows that the surface Co concentrations for the As and Bs samples are much lower than those of the bulk. On a contrary, the Co compounds in the Cs samples are mainly deposited on the outer surface of HZSM-5, which causes a narrower pore mouth. The preferential deposition of Co on the outer surface of the zeolite for the Cs samples may partly due to the size of the $Co(CH_3COO)_2$ complex with a structure as:
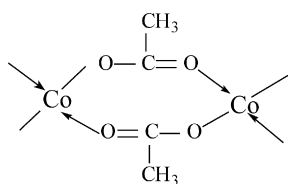
Another reason is the hydrolysis of $Co(CH_3COO)_2$ during impregnation, resulting in the deposition of $Co(OH)_2$ directly on the external surface, and leading to pore mouth narrowing. Similar explanations have been proposed by several researchers [8,9].

3.2. The acidity

The FTIR spectra after pyridine chemisorption of the as-received HZSM-5 and the modified As samples are presented in Fig. 1 (left). Pyridine chemisorption on Brönsted acid sites results in an IR band at $1550 \, cm^{-1}$. A band due to pyridine on Lewis acid sites is observed at $1450 \, cm^{-1}$. The total number of Brönsted acid sites decreased only slightly along with the increase of the Co content, while the amount of Lewis acid sites increased significantly.

The NH_3–TPD curves of the samples are drawn in Fig. 1 (right). The desorptogram of the parent zeolite shows two well resolved peaks at 503 K, denoted as LT peak, and at 723 K, denoted as HT peak, indicating that two types of adsorption sites for NH_3 exist on the surface. The profiles of the As samples are similar to that of the HZSM-5. A trend is observed that the HT peak moves to lower temperature and the LT one shifts to higher temperature with the increase of the Co content. The amount of NH_3 released for the HT peak decreases gradually, while the LT peak increases with the increases of Co content. The total amount of NH_3 released for the samples containing Co is larger than that of the HZSM-5 zeolite. The changes of the amounts of strong acid sites and weak acid sites on the modified samples show some relationship to that of the amount of the Brönsted acid sites and Lewis acid sites. It is plausible that the Brönsted sites are correlated with strong acid sites and the Lewis sites depend on the weak acid sites.

The pyridine FTIR spectra of HZSM-5, A3, B3 and C3 are depicted in Fig. 2. Compared to the parent HZSM-5, an obvious increase of the concentration of the Lewis sites and a slight decrease of that of the Brönsted sites are observed for all the Co containing samples. It shows an order of A3 > B3 > C3 for both the increase and the decrease. The NH_3–TPD curves are
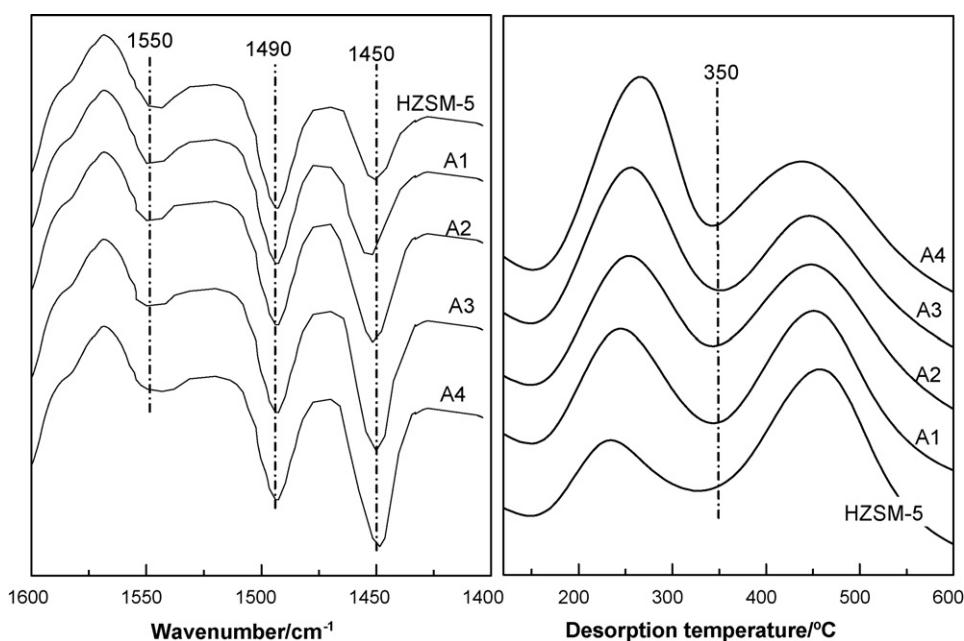

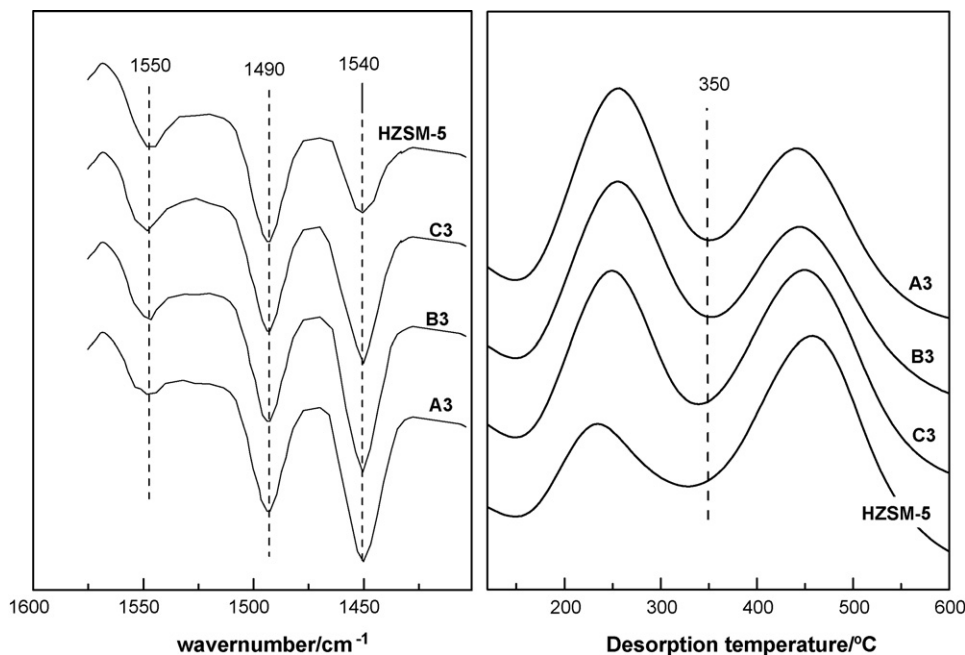Fig. 1. IR spectra of adsorbed pyridine and NH_3–TPD profiles of the sample As.

Fig. 2. IR spectra of adsorbed pyridine and NH_3–TPD profiles of catalysts.

shown in Fig. 2 (right). Compared to the parent HZSM-5, for the cobalt doped samples, it is observed again that, the HT peaks move to lower temperature and the LT peaks shift to higher temperature, while the amount of strong acid sites decreased and that of the weak acid sites increased, with the total amount acid sites increased. It shows similar orders of increase and decreased for the samples with that observed from FTIR. It is obvious that the Co having a strong interaction with the zeolite has a strong effect on the acidity and the effect is enhanced with the increase of Co content. It can be postulated that the ion exchanged Co takes a major role to the modification effect on the acid sites, and the deposited Co as oxide takes effect in pore blocking.

3.3. Catalytic activity

The catalytic performances of the samples were tested in pyridine and picolines synthesis from aldehyde-ammonia condensation under specific conditions. Besides the expected components, the byproducts, such as substituted pyridines as
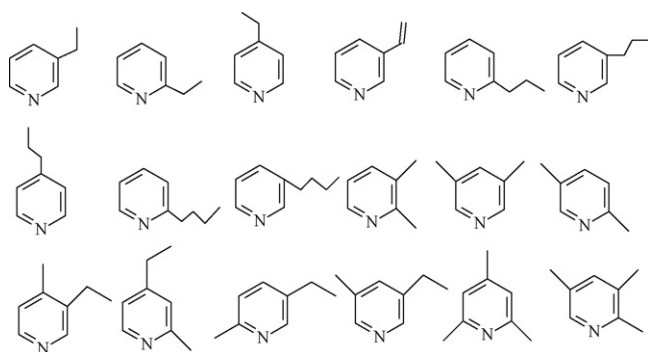

Fig. 3. Byproducts of substituted pyridine.

shown in Fig. 3 and very small amount of benzene derivatives, were observed in the reaction mixture. The byproducts mentioned above were defined as heavy product in activity calculations.

In the data presented in Table 4, the yields of the desired products including pyridine, 2-picoline, 3-picoline and the above mentioned heavy-products are calculated by total carbon balance. The comparative selectivity was actually the data assuming the sum of the selectivities of the three main products and heavy-products as 100%.

The data in Table 4 show that all the modified catalysts give higher yields than the parent HZSM-5. For the different series, the total yields show similar profiles with the increase of Co content, in which a maxima exists. Generally speaking, the increase of product yields could be attributed to two factors, one is the high reactant conversion and the other is the high desired product selectivity. The selectivities of the desired products and heavy-products have no significant improvements for As and Bs samples compared to those of the original zeolite. This is likely parallel to the adsorption results of p-/m-cresols. For the As and Bs samples, metal cations introduced did not result in a blocking of the channel and the narrowing of the pore-mouth. It is logical to think that the higher product yields are mainly due to the higher reactant conversion, instead of the increase of the shape selectivity to desired products. The high reactant conversion may be related to the redistribution and enhancement of the acid sites. Singh et al. proposed a mechanism [10], from which it can be deduced that the increase of the Lewis acid sites and the amount of weak acid sites is of advantage to the activation of ammonia and the formation of intermediate amine and vinyl alcohol, while the decrease of the amount and the strength of strong acid sites is in favor of product desorption. The maximum total yields over the As and Bs samples are 61.3% and 56.1%, respectively. A2

Table 4
Effect of the preparation method on the performance in aldehyde-ammonia condensation reaction

Catalysts	Yield (%)				Comparative selectivity (%)			
	PY	2-MP	3-MP	Total $\sum(PY + 2 - MP + 3 - MP)$	PY	2-MP	3-MP	H-P
HZSM-5	42.4	0.9	7.2	50.5	73.0	1.5	12.4	13.0
A1	43.4	1.4	7.4	52.2	72.2	2.3	14.3	13.2
A2	50.7	1.9	8.7	61.3	72.5	2.7	12.3	12.5
A3	48.9	2.5	8.4	59.8	71.3	3.7	12.2	12.8
A4	46.0	2.6	7.8	56.4	71.7	4.0	12.3	12.0
B1	42.1	1.2	7.0	50.3	73.2	2.1	12.2	12.5
B2	42.7	1.4	7.4	51.5	73.1	1.9	12.7	11.8
B3	45.7	1.6	8.8	56.1	71.7	2.6	13.7	12.0
B4	43.6	1.7	8.6	53.9	70.3	2.8	13.8	13.1
C1	45.5	1.3	7.9	54.7	73.6	2.1	12.8	11.5
C2	47.7	1.4	8.0	57.1	76.6	2.3	12.8	8.3
C3	55.2	2.0	10.7	67.9	77.1	2.8	14.9	5.2
C4	49.6	2.1	9.5	61.2	78.3	3.4	15.0	3.3

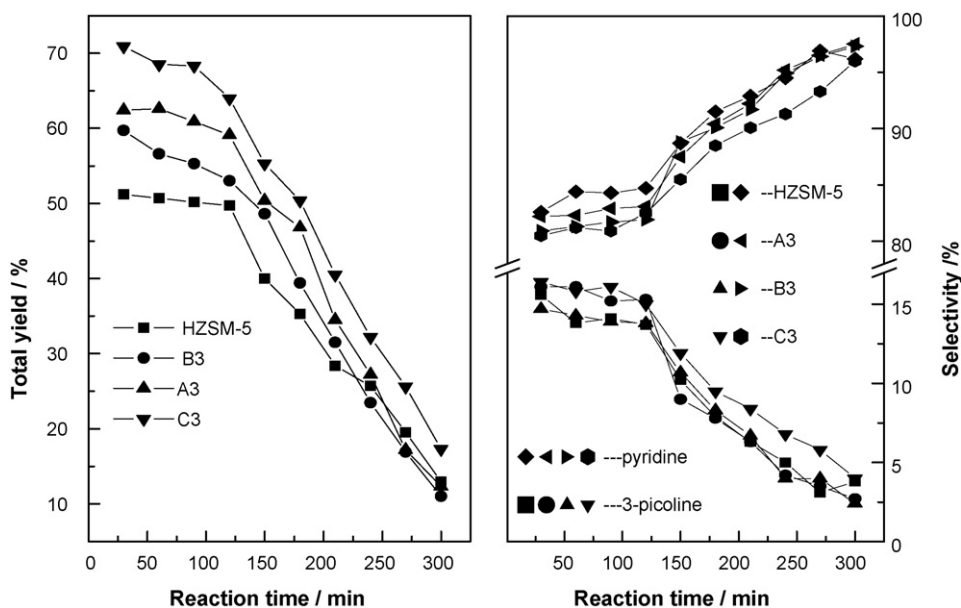PY: pyridine; MP: methyl pyridine; H-P: heavy-products.

Fig. 4. Stability of selected samples.

reaches the maximum at 0.51% Co content, while B3 requires 1.04% Co.

The Cs samples show higher yield, with a maxima of 67.9%, than the other two series of samples. As mentioned above, the redistribution of the acid sites enhances the reactant conversion. Another factor is the obvious shape selectivity to pyridine and picolines. The selectivity of heavy-products showed a gradual decrease from 11.5 to 3.0%, while that of pyridine and picolines increased with the increase of Co content. A pore-mouth narrowing effect is assumed to account partly for this improvement. The kinetic diameter of most byproducts exceeds that of *m*-cresol while that of pyridine and picolines is similar to that of *p*-cresol. Reduction of the pore-mouth restricts selectively the formation of big molecules during the reaction.

Since samples A2, B3 and A3 show the best yields in their own series, the three catalysts are selected for a stability test. The results are shown in Fig. 4. For all the four catalysts examined the yields of pyridine and picolines do not change much in around 2 h, but a rapid decrease was observed afterwards. The yields over A2 and B3 catalysts are close to that over HZSM-5 zeolite. The activity of C3 has a much higher starting point and decreases relatively more slowly. The selectivity of pyridine and 3-picoline show rather constant in 2 h, then a quick increase in pyridine selectivity and a decrease in 3-picoline occurred.

4. Conclusions

Catalysts As were prepared via ion-exchange and Cs were prepared via incipient impregnation methods by using a $Co(CH_3COO)_2$ precursor. The Bs samples were produced by incipient wetness impregnation with a $Co(NO_3)_2$ aqueous solution. The analysis of N_2 adsorption and the separation of *p*-cresol and *m*-cresol measurement show that there is no obvious change

of the pore structure for the As samples and there might be a narrowing of the pore channels and a decrease of pore volume in the Bs samples. However, a narrowing of the pore-mouth is observed for the Cs samples. The measurements of NH_3–TPD and pyridine-IR demonstrate that the highest dispersion and adjustment to the surface acidity is found in the As samples, while the least in the Cs samples among the three series of catalysts. In the aldehyde-ammonia condensation reaction, the order of the desired products yield is the samples Cs > the samples As > the samples Bs with a same Co content and all these modified samples give better yield than the unmodified HZSM-5 zeolite. The effects of Co on the catalytic activity are mainly attributed to the modification of surface acidity and the shape selectivity due to the narrowing of the pore mouth.

Acknowledgement

References

[1] S.E. Golunski, D. Jackson, Appl. Catal. 23 (1986) 1.
[2] S.J. Kulkanrni, R. Ramachandra Rao, M. Subrahmanyam, A.V. Rama Rao, Appl. Catal. A 113 (1994) 1.
[3] A.V. Rama Rao, S.J. Kulkanrni, R. Ramachandra Rao, M. Subrahmanyam, Appl. Catal. A 111 (1994) 101.
[4] N. Srinivas, V. Radha Rani, S.J. Kulkarni, K.V. Raghavan, J. Catal. 208 (2002) 332.
[5] R.M. Dessau, U.S. Patent 5,350,504 (1994).
[6] S. Shimizu, N. Abe, U.S. Patent 4,810,794 (1989).
[7] M. Saitoh, Y. Tanaka, U.S. Patent 5,952,258 (1999).
[8] J. Wang, B.J. Zhao, Y.C. Xie, Acta Phys. Chim. Sin. 17 (2001) 966.
[9] W. Zou, D.Q. Yang, Z. Gao, Chin. J. Catal. 26 (2005) 470.
[10] B. Singh, S.K. Roy, K.P. Sharma, J. Chem. Technol. Biotechnol. 71 (1998) 246.